Nuclear Engineering and Technology 48 (2016) 711–718

Available online at ScienceDirect

Nuclear Engineering and Technology

journal homepage: www.elsevier.com/locate/net

Original Article

Study of Lower Hybrid Current Drive for the Demonstration Reactor

Ali Asghar Molavi-Choobini [a,*], *Ahmad Naghidokht* [b], *and Zahra Karami* [c]

[a] *Department of Physics, Faculty of Engineering, Islamic Azad University, Shahr-e-kord Branch, Shahr-e-kord, Iran*
[b] *Department of Physics, Urmia University, Urmia, Iran*
[c] *Department of Engineering, Islamic Azad University, Zanjan Branch, Zanjan, Iran*

ARTICLE INFO

Article history:
Received 28 November 2014
Received in revised form
21 December 2015
Accepted 18 January 2016
Available online 26 February 2016

Keywords:
Current Drive
Demonstration Reactor
Fokker–Planck Equation
Lower Hybrid Waves

ABSTRACT

Steady-state operation of a fusion power plant requires external current drive to minimize the power requirements, and a high fraction of bootstrap current is required. One of the external sources for current drive is lower hybrid current drive, which has been widely applied in many tokamaks. Here, using lower hybrid simulation code, we calculate electron distribution function, electron currents and phase velocity changes for two options of demonstration reactor at the launched lower hybrid wave frequency 5 GHz. Two plasma scenarios pertaining to two different demonstration reactor options, known as pulsed (Option 1) and steady-state (Option 2) models, have been analyzed. We perceive that electron currents have major peaks near the edge of plasma for both options but with higher efficiency for Option 1, although we have access to wider, more peripheral regions for Option 2. Regarding the electron distribution function, major perturbations are at positive velocities for both options for flux surface 16 and at negative velocities for both options for flux surface 64.

1. Introduction

Lower hybrid current drive (LHCD) is used in a large number of present day tokamaks in order to extend the length of operating pulses beyond what is possible with inductive current drive. Since the absorption of LHCD waves takes place away from the center of the plasma, LHCD also produces a modification of the current profile, which is useful in order to improve the stability of the machine. A major objective of research on current drives in the longer term is to find a way of driving a tokamak reactor in a steady state, while keeping the level of power that has to be recirculated back into the reactor within reasonable bounds.

One of the most crucial and challenging issues of the fusion power plant is the development of reactor scenarios that simultaneously satisfy the requirements of sufficiently high power amplification with the need for a sustainable power exhaust. The main options based on the above issue can also

* *Corresponding author.*
E-mail address: Aliasghar.molavi64@gmail.com (A.A. Molavi-Choobini).
http://dx.doi.org/10.1016/j.net.2016.02.003

be used to design the demonstration reactor (usually called DEMO) which, with respect to commercial power plants, is downscaled to an electrical power production of the order of 1 GW [1]. The DEMO project is currently at the conceptual design stage and consequently, no final configuration is defined. DEMO is hoped to be able to confirm the technological feasibility of fusion power and demonstrate its commercial viability. DEMO will be the first fusion device to export significant amounts of electrical power from fusion [2].

There are two distinct mechanism for the absorption of lower hybrid (LH) waves, one of which, electron Landau damping, is a very effective current drive mechanism. The other mechanism, stochastic ion heating, is not useful for current drive. Most LHCD experiments run in a regime where the wave frequency is above the LH frequency everywhere in the plasma, so the only damping mechanism is Landau damping. Landau damping is favored at low densities and above a certain density threshold there is a transition to ion heating. Also in the regime in which the current drive is effective, nonlinear effects such as parametric decay processes do not appear to play an important role [3].

LH waves have the attractive property of damping strongly via electron Landau resonance on relatively fast tail electrons at (2.5–3) $\times$ v_{Te}, where $v_{Te} = \sqrt{\frac{2T_e}{m_e}}$ is the electron thermal speed. Consequently these waves are well-suited to driving current in the plasma periphery where the electron temperature is lower, making LHCD a promising technique for off-axis $\left(\frac{r}{a} \geq 0.6\right)$ current profile control in reactor grade plasmas. Indeed off-axis LHCD has already been shown to be an effective tool for optimizing the current profile for access to advanced tokamaks operating modes in JET [4] and JT-60U [5] tokamaks. In addition the RF source frequency can be chosen to be high enough to minimize the parasitic interaction of LH waves with fusion-generated α particles. The relatively high phase speed also minimizes deleterious effects due to particle trapping, which can become important in the periphery. LH waves have been successfully utilized for electron and ion plasma heating, to sustain and ramp-up toroidal plasma current, and to stabilize sawteeth in tokamaks [6]. Current carrying fast electrons are generated by LH waves through parallel electron Landau damping when the resonance condition is fulfilled. Experiments in many tokamaks such as Tore Supra [7], TRIAM-IM [8], FTU [9], JET [10], JT-60U [11], and HT-7 [12] have shown that LHCD is one of the most efficient methods to drive noninductive current in tokamak plasmas. In order to conduct the analysis of the electron distribution function, we must use a one-dimensional Fokker–Planck equation. Axial symmetry around the magnetic field allows the reduction in the complexity of the problem from three to two velocity dimensions. The reduction of velocity dimension from two to one is made under the assumption of the dependence of the electron velocity distribution function on the perpendicular velocity that supposes the electron temperature as a Maxwellian distribution [13]. For the current drive, waves with adequate phase velocity are injected along the toroidal magnetic field to resonate with plasma electrons and raise the energy and momentum of the electrons by the absorption of wave energy with Landau damping. The solution of the Fokker–Planck equation on each flux surface gives the electron distribution function, and hence the current density, on that flux surface. The mechanism is straightforward Landau damping and the experiments are well explained by a balance between wave diffusion of the particles, described by a standard quasilinear term, and collisional slowing down and velocity space diffusion, described by a Fokker–Planck collision term.

The outline of the paper is as follows: in Section 2 we write the Fokker–Planck equation with an additional quasilinear diffusion term that describes the interaction of the waves with the plasma. In Section 3 we present a numerical solution method for the Fokker–Planck equation in brief and we simulate several parameters associated with the lower hybrid wave injection (electrons current, electron distribution function, and phase velocity changes) for two options of DEMO. Option 1 is the DEMO pulsed model, where a transformer drives the main current, and Option 2 is related to *optimistic* DEMO design, pointing at steady-state operations that are at the upper limit of achievable International Thermonuclear Experimental Reactor (ITER) performance. Option 2, compared to its consecutive counterpart (Option 1), entails the most demanding challenges that the fusion community may expect in LHCD system in the coming years [14].

2. Fokker–Planck equation

With increasing energy of plasma particles, Coulomb collisions of plasma particles with each other increase. The effect of such collisions is obtained by adding a quasilinear term to the Vlasov equation, which is called the Fokker–Planck equation and gives a general description of the distribution function changes due to successive collisions. The rate of change of distribution function f due to collisions can be written as:

$$\left(\frac{\partial f}{\partial t}\right)_{coll} = \sum_s \frac{4\pi n_s q_T^2}{m_T^2} \left\{ -\frac{\partial}{\partial v_i}\left(f_T \frac{\partial H_s}{\partial v_i}\right) + \frac{1}{2}\frac{\partial^2}{\left(\partial v_i \partial v_j\right)}\left(f_T \frac{\partial^2 G_s}{\partial v_i \partial v_j}\right) \right\} \quad (1)$$

in which n_s is the density of typical particles (electrons or ions), q_T is the charge of the test particle, m_T is the mass of the test particle, f_T is the distribution function of test particles, and v_i is the velocity of particle type i. Functions $G_s(v)$ and $H_s(v)$ are auxiliary functions and can be defined as follow:

$$G_s(v) = \int f_s(v')\left(v_T - v'\right)dv' \quad (2)$$

$$H_s(v) = \int f_s(v')\frac{\left(v_T - v'\right)}{\left|\mathbf{v}_T - \mathbf{v}'\right|^3}dv' \quad (3)$$

These describe diffusion coefficients are caused by velocity changes in the phase space [15].

2.1. Solving method of Fokker–Planck equation

In a strong magnetic field, the electron distribution function has cylindrical symmetry in velocity space, so the problem

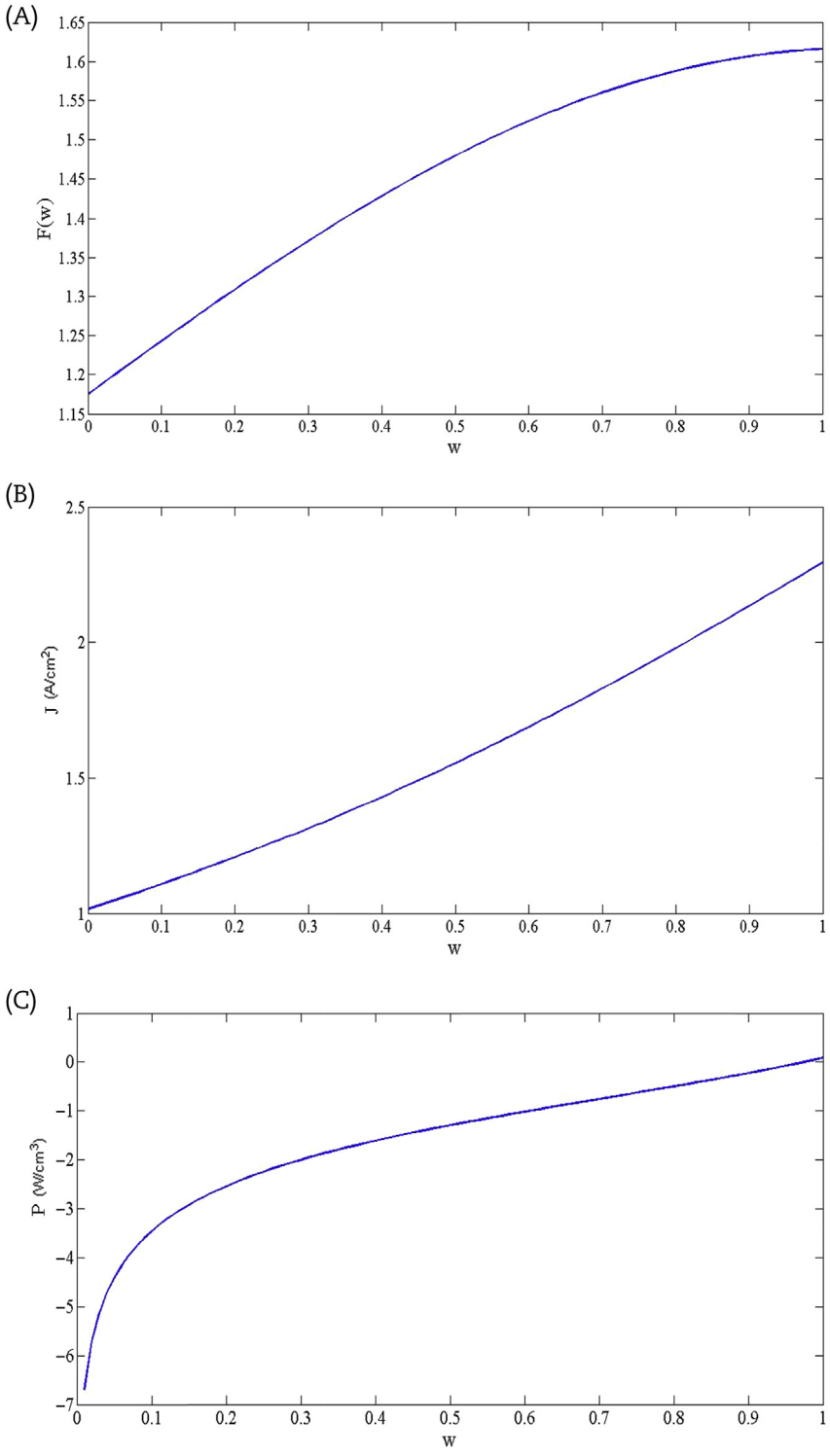

Fig. 1 – (A) Distribution function F(w); (B) current function, and (C) power function P of tritium plasma.

becomes that of solving a two-dimensional (2D) partial differential equation. In order to run the calculation in a reasonably short time, various approximations are built in. The most important is the use of a Fokker–Planck equation, which is one dimensional (1D) in velocity space. With regard to particle acceleration by waves, the LHCD has been shown to be a very effective method of accelerating electrons along the magnetic field lines in a tokamak. The mechanism is straightforward Landau damping. Fast electrons have a high probability of pitch-angle scattering into the reverse direction and running away. A runaway electron drains energy out of the electric field, leading to a degradation of the ramp-up efficiency. In fact, there is a distortion of electron distribution function due to pitch-angle scattering of electrons into the

perpendicular direction. The LH waves simulation code (LSC) does not have improper treatment of 2D velocity space effects in the wave absorption, in particle trapping and bounce averaging of the RF operator. We should note that analysis based on a 1D Fokker–Planck equation does not predict the important physical phenomenon of RF-generated reverse runaways [16]. The 2D velocity space treatment is included completely in some codes such as CQL3D [17,18] and DELPHINE [19]. The LSC model attempts to account for 2D velocity space effects in the dissipated power by replacing the leading coefficient $\left(\frac{(2+Z_{eff})}{2}\right)$ of the collision operator C with $\left(\frac{(1+Z_{eff})}{5}\right)$ [20]. Now we shall consider uniform plasma initially at equilibrium. For the next time, i.e., $t > 0$, plasma is subject to an electric field $\mathbf{E}(t)$ and a wave-induced flux $\mathbf{S}(\mathbf{v},t)$. If the electric field and the wave-induced flux are weak enough, the electron distribution remains close to a Maxwellian distribution for $\xi \leq T$, where $\xi = \frac{1}{2}mv^2$ is the energy of an electron. We shall take the ions to be infinitely massive so that they form a stationary background off which the electrons collide. Substituting $f_m + f_1$ into the Boltzmann equation for the electron distribution f and linearizing then gives:

$$\frac{\partial f_1}{\partial t} + \frac{q\mathbf{E}(t)}{m}\cdot\frac{\partial}{\partial \mathbf{v}}f_1 - C(f) = -\frac{\partial}{\partial \mathbf{v}}\cdot\mathbf{S} - \frac{q\mathbf{E}(t)}{m}\cdot\frac{\partial}{\partial \mathbf{v}}f_m - \left[\frac{\dot{n}}{n} + \left(\frac{\xi}{T} - \frac{3}{2}\right)\frac{\dot{T}}{T}\right]f_m \tag{4}$$

where

$$f_m = n\left(\frac{m}{2\pi T}\right)^{\frac{3}{2}}\exp\left(-\frac{\xi}{T}\right) \tag{5}$$

is Maxwellian distribution and $C(f) = C(f, f_m) + C(f_m, f) + C(f, f_1)$ is linearized collision operator [16] and comes in the form of:

$$C(f) = \Gamma\left(\frac{1}{v^2}\frac{\partial f}{\partial v} + \frac{1+z}{2v^3}\frac{\partial}{\partial \mu}(1-\mu^2)\frac{\partial}{\partial \mu}f\right) \tag{6}$$

where $\mu = \frac{v_\parallel}{v}$, $\Gamma = -\frac{eq^4\ln\Lambda}{4\pi m^2\varepsilon_0^2}$, ε_0 is the dielectric constant of free space, $\ln\Lambda$ is the Coulomb logarithm, and Z is the effective ion charge state. In Eq. (4), q, m, n, and T are the electron charge, mass, number density, and temperature, respectively. Normally a linearized form of the collision operator is used, in which the fast particles collide with a predetermined background distribution. With convenient normalization, Eq. (1) then becomes:

$$\frac{\partial f_1}{\partial \tau} + D(f_1) = -\frac{\partial}{\partial \mathbf{u}}\cdot\mathbf{S} \tag{7}$$

With $f_1(\mathbf{u}, \tau = 0) = 0$ and the operator D defined by [21]:

$$D = -\frac{\partial}{\partial \mathbf{u}_\parallel} - \frac{1}{u^2}\frac{\partial}{\partial \mathbf{u}} + \frac{1+z}{2u^3}\frac{\partial}{\partial \mu}(1-\mu^2)\frac{\partial}{\partial \mu} \tag{8}$$

Then the evolution of the electron distribution function,f, in the presence of RF waves, is given by:

$$\frac{\partial f}{\partial t} = \frac{\partial}{\partial v_\parallel}D_{RF}(v_\parallel)\frac{\partial}{\partial v_\parallel}f + \left(\frac{\partial f}{\partial t}\right)_{coll} \tag{9}$$

where, $v_\parallel$ is the velocity parallel to the magnetic field, $D_{RF}(v_\parallel)$ is the quasilinear diffusion coefficient, and $\left(\frac{\partial f}{\partial t}\right)_{coll}$ is the Fokker–Planck collision term. The wave diffusion of particles is represented by standard quasilinear term. Again normalizing velocities to $v_{Te} = \left(\frac{T_e}{m_e}\right)^{\frac{1}{2}}$ and time $v_0^{-1}\left(v_0 = \frac{\log\Lambda\omega_{pe}^4}{2\pi n_0 v_{Te}^3}\right)$, Eq. (9) becomes:

$$\frac{\partial f}{\partial \tau} = \frac{\partial}{\partial w}D(w)\frac{\partial}{\partial w}f + \left(\frac{\partial f}{\partial \tau}\right)_{coll} \tag{10}$$

where $\tau = v_r t$, $w = \frac{v_\parallel}{v_{Te}}$, and $D(w) = \frac{D_{RF}(v_\parallel)}{(v_{Te}^3 v_0)}$. v_r is the running velocity of electrons, i.e., the velocity at which collisional frictional force equals the acceleration caused by the electric field. Also, we define a runaway collision frequency as: $\nu_r \equiv \frac{\Gamma}{|v_r|^3}$ [22]. Since driving frequency ω is small in comparison to the electron gyro frequency Ω_e, the current drive mechanism for LH waves are utilized only in the resonance of parallel wave phase velocity $\left(\frac{\omega}{k_\parallel}\right)$ and the quasilinear diffusion tensor reduces to the term, $v_\parallel v_\parallel$. Moreover, in general, the wave spectrum may be of arbitrary shape. However, we can partially solve the problem by considering very large spectrum amplitudes and anticipate that the precise wave amplitude is immaterial due to the wave saturation, and so ignore it. This assumption is strictly valid when $v_\perp \ll \frac{\Omega_e}{k_\parallel}$. Thus:

$$D(w) = \begin{cases} D & for\ w_1 < w < w_2 \\ 0, & otherwise \end{cases} \tag{11}$$

where the constant, D, is chosen to be large enough for the solution to be insensitive to its precise magnitude. This is, in fact, what occurs in situations of interest such as RF heating or RF-driven tokamak reactors [22,23]. Thus, in summary, we have pinpointed the important free parameters in the problem as just two: w_1 and w_2, maximum and minimum parallel phase velocities of LH injection waves which were normalized to the electron heating velocity and characterize the resonance area of LH injection waves. Solving that equation for the steady-state distribution, gives:

$$F(w) = C\exp\left(\int^w \frac{-w dw}{1 + 2w^3\frac{D(w)}{(2+z)}}\right) \tag{12}$$

where, C is a constant in integration and $F(w)$ has been plotted in Fig. 1A for $D(w) = ½$ and $Z = 3$, i.e., for tritium plasma. Using this distribution function and its normalized velocity component that will be $F(w)$, we can obtain power and current as in [16] and [22]:

$$P = \int \frac{wD(w)(\partial F(w))}{\partial w}dw = \frac{z+2}{2}\frac{\exp\left(\frac{-w_1^2}{2}\right)}{(2\pi)^{\frac{1}{2}}}\log\left(\frac{w_2}{w_1}\right) \tag{13}$$

$$J = \int wF(w)dw = \frac{\exp\left(\frac{-w_1^2}{2}\right)}{(2\pi)^{\frac{1}{2}}}\Delta\left(\frac{w_1+w_2}{2}\right) \tag{14}$$

Here we obtained equations J and P by using a numerical method for tritium plasma and plotted them in Figs. 1B and 1C in order to characterize current drive and power transferred in a plasma environment and to show the efficiency of this method.

3. Simulation and results

The LSC is a computational model for LH waves current drive based on the FORTRAN programming language, in which electrons and ions heating, geometric details and plasma profile are discussed and space effects of the 2D phase of the wave spectrum injected in Fokker–Planck equation is approximated in order to simulate the desired parameters. The LSC suite is based on a set of mutually coupled codes consisting of a ray-tracing tool and a quasilinear Fokker–-Planck code. The LH wave propagation module is based on multiple ray tracing in axisymmetric plasmas of an arbitrary cross section. Absorption of RF power is estimated by computing flux surface averaged quasilinear damping in one velocity space dimension. The ray information with an assumption of low power and linear damping is used to form an estimate of the quasilinear diffusion coefficient averaged on each flux surface. Then, an electron velocity distribution is obtained by solving a 1D Fokker–Planck equation with the DC electric field set to zero. The power level raised gradually while the distribution function, power deposition and quasilinear diffusion coefficient are iteratively recomputed. After this has been done, a driven current, which depends on the local electric field, is calculated from the results of the adjoint method of Karney and Fisch [17]. The LSC code [24] employs a Green's function treatment [25] of the Fokker–Planck equation from which the driven current is formulated by convolving the resulting response function (χ) with the wave induced RF flux (Γ_{rf}):

$$J_{rf} = \int d^3p \frac{\partial \chi}{\partial p} . \Gamma_{rf}, \quad \Gamma_{rf} = -D_{ql} \frac{\partial f_e}{\partial p_{\parallel}} \tag{15}$$

This approach is computationally fast and the response function (χ) includes 2D velocity space effects, particle trapping and momentum conserving corrections in the collision operator. However, the method relies on an estimate for the wave induced RF flux, which is computed in LSC from a 1D parallel velocity space solution of equation [26].

We have two types of input files in LSC. The first file, input.lhh, which must always be present, contains information about rays, velocity grids, computing, and plotting options. The second file, input.xry, which does not have to be present, contains information about the X-ray camera.

The LSC that we have used here is approximated to 1D (parallel to the magnetic field); and for accessing better results, perpendicular temperature must be considered too. We have related parameters of two options of DEMO in [14]. In this paper, we traced 15 rays and electron distribution functions, electrons current, and phase velocity changes are simulated and are plotted by computational software of MATLAB by using the LSC program.

Here we choose the injection of 5 GHz LH waves. The choice of LHCD frequency results from a delicate trade-off between manifold counteracting elements: several physics issues demand to move the frequency as high as possible, while technological limitations put some upper bounds. Some mechanisms also entail deleterious effects for LHCD [27]. Referring to the simulations performed for different ITER scenarios shows that accordingly, albeit no calculations have yet been carried out for DEMO, an LHCD system for this machine can be hardly conceived with a frequency lower than 5 GHz. Also, given a certain power to be launched through a port, a multipactor also constrains the operational frequency. Coming to technological issues, 5 GHz currently represents the highest frequency that suitable, reliable, high power RF sources (i.e., klystrons) are expected to achieve in a reasonable time. Alternatively the 4.6 GHz, 250 kW klystrons developed, represent a back-up solution. Although 5 GHz sources are not fully developed, and the location of DEMO together with its alternating current distribution grid is not known, a solution close to the one proposed for ITER can be reasonably envisaged. We have LH frequencies that are suitable for specific tokamaks such as FTU (8 GHz), Alcator C-mode (4.6 GHz), EAST (2.45 GHz), JET (3.7 GHz), Tore Supra (3.7 GHz), KSTAR (5 GHz), and 5 GHz proposed in ITER (accordingly for DEMO) [28].

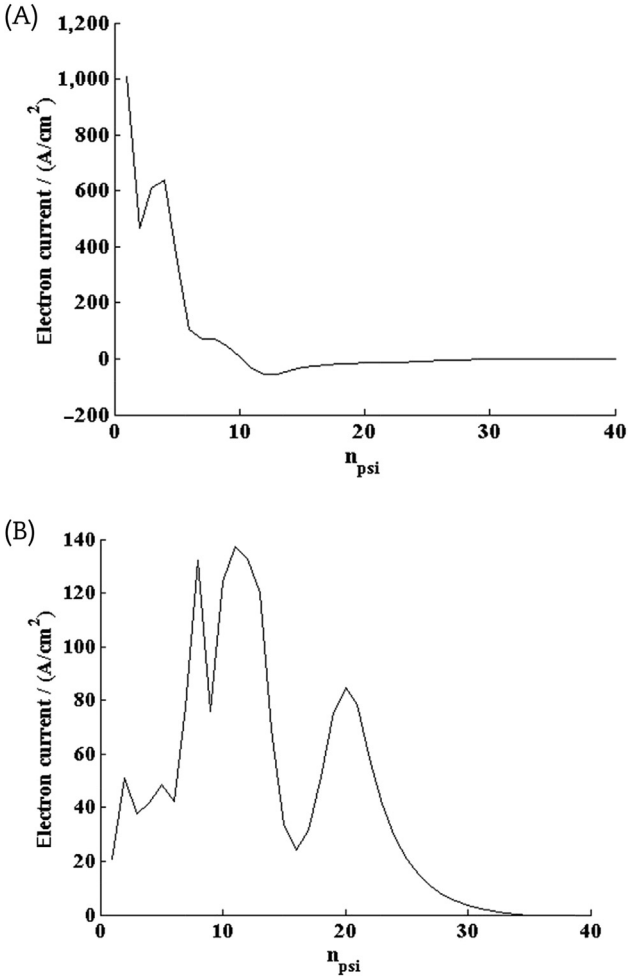

Fig. 2 – Electrons current at the number of flux surfaces for demonstration reactor. (A) Option 1 and (B) Option 2.

3.1. *Electrons current*

Applying an electric field to the tokamak plasma environment, causes the separation of charged particles. This charge separation causes an electric current in the plasma environment that is called the bootstrap current. Furthermore,

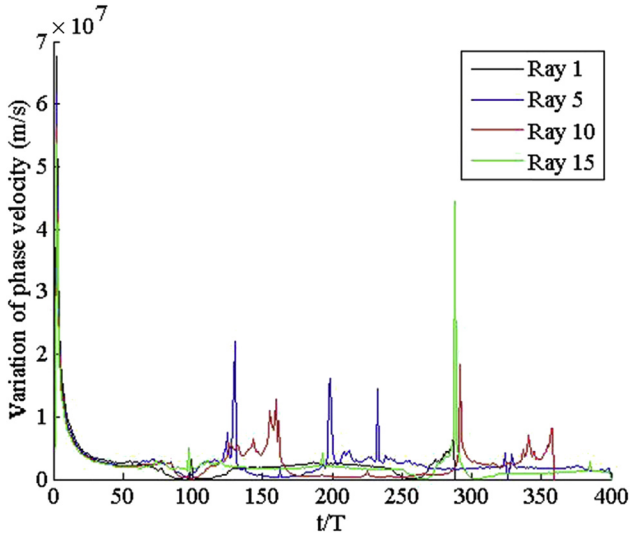

Fig. 3 – Phase velocity changes of the lower hybrid beams injected into plasma at time normalized to the injected wave frequency period.

launching a wave into the plasma environment, the plasma electrons produce an electron current by receiving the momentum and energy of the wave. To simulate the electrons current in tokamak, we divide plasma into 40-flux surfaces of injected wave (actually in LSC, 40 is the maximum number of toroidal components of $n_{\|}$) and plot these parameters at the flux surfaces. Electron currents are obtained with this equation [22]:

$$J_{rf} = \frac{-en_e}{\Gamma}\int d\upsilon_{\|} D_{RF}(\upsilon_{\|})\frac{\partial f_e(\upsilon_{\|})}{\partial \upsilon_{\|}}\frac{4\upsilon_{\|}^3}{5+z}\left[\mu - \frac{1+z/2+3\mu^2/2}{3+z}\frac{\upsilon_{\|}^2}{\upsilon_r^2}\right] \tag{16}$$

Electron currents are plotted in Fig. 2 for two options of DEMO. As shown in Fig. 2A, the maximum electron current for DEMO Option 1 is located at the plasma edge and has a negative value at the next flux surfaces and then reaches zero at the plasma center. The negative case would be justified since the electron current at such surfaces is in the opposite direction of the bootstrap current. For Option 2 (Fig. 2B), the maximum electron current is located both at the plasma edge and near the flux surfaces of mid-plane plasma (approximately in more peripheral regions) and has lower efficiency compared to Option 1, as in the results from [29].

3.2. *Phase velocity changes*

Thermal effects added to cold plasma should be considered because there are particles that move at speeds approaching phase velocity in a heat distribution. Such particles have resonant interaction with waves and their interaction results in wave damping and instability. The waves with $k_{\perp} = 0$, are not affected by the magnetic field and resonance does not happen. Moreover, for such waves, we have cut-off in $\omega = \omega_p$. For waves with $k_{\perp} = 0$, the dispersion relation of electro dynamic waves for collision plasma along the magnetic field is presented by:

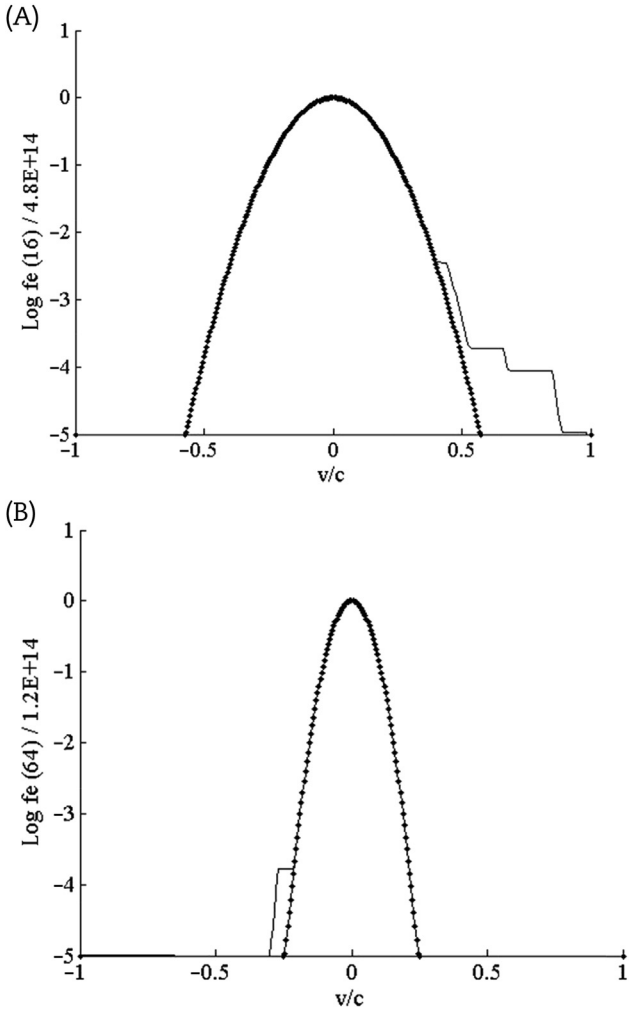

Fig. 4 – Electron distribution function for flux surfaces. (A) 16 and (B) 64 for demonstration reactor Option 1.

$$\frac{k^2c^2}{\omega^2} = 1 - \frac{\omega_{pe}^2}{\omega^2}\frac{1}{\left(1 \mp \frac{\omega_{ce}}{\omega} - \frac{\omega_{ce}\omega_{ci}}{\omega^2}\right)} \tag{17}$$

According to the dispersion relation, the equation of the injected wave phase velocity that is propagated along the magnetic field is changed as:

$$\upsilon_{ph} = c\left(1 - \frac{\omega_{pe}^2}{\omega^2}\left(\frac{1}{1 \mp \frac{\omega_{ce}}{\omega}}\right)\right)^{\frac{-1}{2}} \tag{18}$$

We simulated particle phase velocity changes in order to inject the LH waves into plasma in DEMO Option 2 and plotted it for five beams with different frequencies in Fig. 3. Resonant regions for each ray in which wave damping occurs and wave energy transfers to the plasma environment have been shown in this diagram as a peak [30].

3.3. *Electron distribution function*

In solving f_e, we set $\partial/\partial t = 0$ because the time for equilibrium between RF power and the electron distribution function is

short compared to the time for plasma to evolve. Then the solution for f_e is an integral in velocity space [31]:

$$f_e(v_\parallel) = \frac{1}{\sqrt{2\pi v_{Te}^2}} \exp\left(- \int_0^{v_\parallel} \frac{v_c(v')v'dv'}{D_c(v') + D_{ql}(v')} \right) \quad (19)$$

We simulated a logarithm of the electron distribution function of two options of DEMO in Figs. 4 and 5 for the frequency of LH wave 5 GHz and at two flux surfaces, 16 and 64. The origin plot (light curve) is referred to the Maxwell distribution function in equilibrium state and we see some tails. If the fast electrons move along the positive $v_\parallel$, they have a chance of being scattered along the negative direction and producing negative currents, such as in Fig. 4B and Fig. 5B, and vice versa. In the LH drive in fusion plasmas, however, the waves will propagate only in one direction and net parallel currents will be considered. Figures of the distribution function show fairly good agreement with the results of [32].

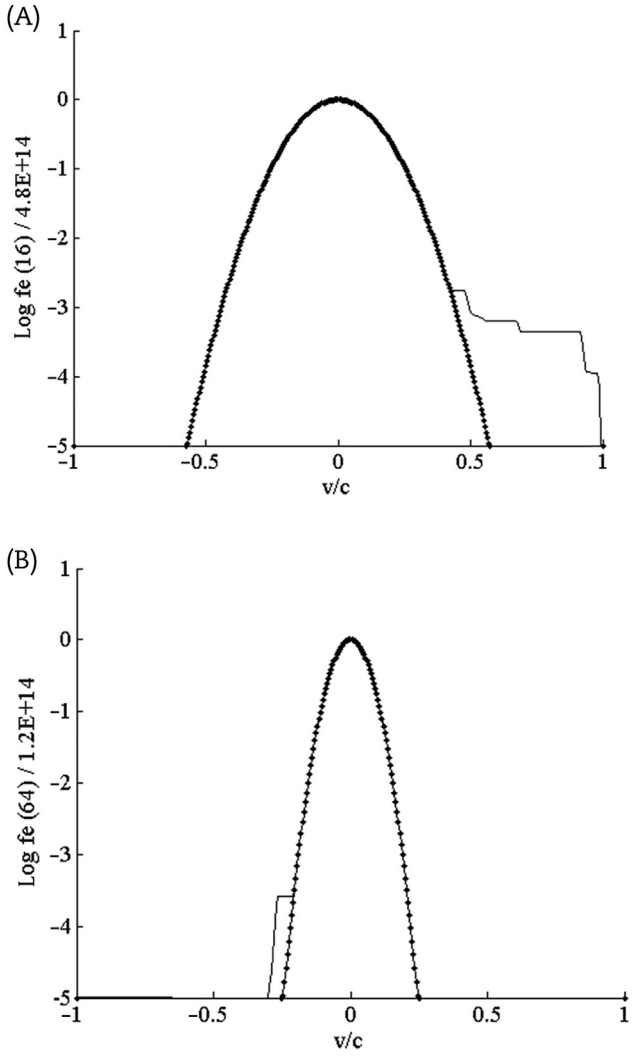

Fig. 5 – Electron distribution function for flux surfaces. (A) 16 and (B) 64 for demonstration reactor Option 2.

4. Discussion

Because of its advantages in terms of simplicity and efficiency, a LHCD has been widely used in tokamak experiments. LHCD has proven to be one of the most efficient ways to generate noninductive current in tokamak experiments. Two plasma scenarios pertaining to two different DEMO options, known as pulsed (Option 1) and steady-state (Option 2) models, have been analyzed. According to results, electron currents, have major peaks near the edge of plasma for both options but with higher efficiency for Option 1, although we have access to wider, more peripheral regions for Option 2. Regarding electron distribution function, major perturbations are at positive velocities for both options for flux surface 16 and at negative velocities for both options for flux surface 64. If the fast electrons move along the positive $v_\parallel$, they have a chance of being scattered along the negative direction and produce negative currents, as shown in Figs. 4B and 5B and vice versa. In the LH drive in fusion plasmas, however, the waves will propagate only in one direction, and net parallel currents will be considered. Our results are approximate since the LSC code that we have used here is approximated to one dimension (parallel to magnetic field) and for accessing better results, perpendicular temperature must also be considered. However, these results give us good insight and are in fairly good agreement with results for ITER [33].

Conflicts of interest

All authors declare no conflicts of interest.

REFERENCES

[1] J. Garcia, G. Giruzzi, J.F. Artaud, V. Basiuk, J. Decker, F. Imbeaux, Y. Peysson, M. Schneider, Analysis of DEMO scenarios with the CRONOS suite of codes, Nucl. Fusion 48 (2008) 075007.

[2] R. Zagorski, R.I. Ivanova-Stanik, R. Stankiewicz, Simulations with the COREDIV code of DEMO discharges, Nucl. Fusion 53 (2013) 073030.

[3] R.A. Cairns, Lower hybrid current drive, Phys. Scripta T50 (1994) 69–74.

[4] F.X. Soldner (The JET Team), Shear optimization experiments with current profile control on JET, Plasma Phys. Control. Fusion 39 (1997) B353.

[5] S. Ide, O. Naito, T. Oikawa, T. Fujita, T. Kondoh, M. Seki, K. Ushigusa, JT-60 Team, LHCD current profile control experiments towards steady state improved confinement on JT-60U, in: Proceedings of the 17th Conference on Fusion Energy. Yokohama (Japan), 1998, p. 567.

[6] P.T. Bonoli, M. Porkalob, Y. Takase, S.F. Knowlton, Numerical modeling of lower hybrid RF heating and current drive experiments in the Alcator C tokamak, Nucl. Fusion 28 (1988) 991.

[7] D.V. Houtte, G. Martin, A. Bécoulet, J. Bucalossi, G. Giruzzi, G.T. Hoang, Th. Loarer, B. Saoutic (on behalf of the Tore Supra Team), Recent fully non-inductive operation results in Tore supra with 6 min, 1 GJ plasma discharges, Nucl. Fusion 44 (2004) L11.

[8] S. Itoh, K.N. Sato, K. Nakamura, H. Zushi, M. Sakamoto, K. Hanada, E. Jotaki, K. Makino, S. Kawasaki, H. Nakashima, N. Yoshida, Recent progress on high performance steady state plasmas in the superconducting tokamak TRIAM-1M, Nucl. Fusion 39 (1999) 1257.
[9] B. Angelini, S.V. Annibaldi, M.L. Apicella, G. Apruzzese, E. Barbato, A. Bertocchi, F. Bombarda, C. Bourdelle, A. Bruschi, P. Buratti, G. Calabrò, A. Cardinali, L. Carraro, C. Castaldo, C. Centioli, R. Cesario, S. Cirant, V. Cocilovo, F. Crisanti, R. De Angelis, M. De Benedetti, F. De Marco, B. Esposito, D. Frigione, L. Gabellieri, F. Gandini, L. Garzotti, E. Giovannozzi, C. Gormezano, F. Gravanti, G. Granucci, G.T. Hoang, F. Iannone, H. Kroegler, E. Lazzaro, M. Leigheb, G. Maddaluno, G. Maffia, M. Marinucci, D. Marocco, J.R. Martin-Solis, F. Martini, M. Mattioli, G. Mazzitelli, C. Mazzotta, F. Mirizzi, G. Monari, S. Nowak, F. Orsitto, D. Pacella, L. Panaccione, M. Panella, P. Papitto, V. Pericoli-Ridolfini, L. Pieroni, S. Podda, M.E. Puiatti, G. Ravera, G. Regnoli, G.B. Righetti, F. Romanelli, M. Romanelli, F. Santini, M. Sassi, A. Saviliev, P. Scarin, A. Simonetto, P. Smeulders, E. Sternini, C. Sozzi, N. Tartoni, D. Terranova, B. Tilia, A. Tuccillo, O. Tudisco, M. Valisa, V. Vershkov, V. Vitale, G. Vlad, F. Zonca, Overview of the FTU results, Nucl. Fusion 45 (2005) S227.
[10] J. Pamela, E.R. Solano, JET EFDA Contributors, Overview of JET results, Nucl. Fusion 43 (2003) 1540.
[11] S. Ide, T. Fujita, O. Naito, M. Seki, Sustainment and modification of reversed magnetic shear by LHCD on JT-60U, Plasma Phys. Control. Fusion 38 (1996) 1645.
[12] J. Liu, X. Gao, L.Q. Hu, M. Asif, Z.Y. Chen, B.J. Ding, Q. Zhou, H.Q. Liu, X.Y. Jie, W. Kong, S.Y. Lin, Y.H. Ding, L. Gao, Q. Xu, The HT-7 Team, Lower hybrid current drive experiment with graphite limiters in the HT-7 superconducting tokamak, Phys. Lett. A 350 (2006) 386.
[13] M.S. Weston, Fusion: An Introduction to the Physics and Technology of Magnetic Confinement Fusion, second ed., Wiley-VCH Verlag GmbH & Co. KGaA, Berlin, 2010, pp. 211–234.
[14] E. Poli, G. Tardini, H. Zohm, E. Fable, D. Farina, L. Figini, N.B. Marushchenko, L. Porte, Electron-cyclotron current drive in DEMO plasmas, Nucl. Fusion 53 (2013) 013011.
[15] A.N. Kral, A.W. Trivelpiece, Principles of Plasma Physics, McGraw-Hill, Baltimore, 2005, pp. 1–440.
[16] N.J. Fisch, Theory of current drive in plasma, Rev. Mod. Phys. 59 (1987) 175.
[17] R.W. Harvey, M.G. McCoy, in: Proceedings of the IAEA Technical Committee Meeting on Advances in Simulation and Modeling of Thermonuclear Plasmas, Montreal, 1992, pp. 489–526.
[18] A.P. Smirnov, R.W. Harvey, Calculations of the current drive in DIII-D with the GENRAY ray tracing code, Bull. Am. Phys. Soc. 40 (1995) 1837.
[19] F. Imbeaux, Y. Peysson, Ray-tracing and Fokker–Planck modelling of the effect of plasma current on the propagation and absorption of lower hybrid waves, Plasma Phys. Control. Fusion 47 (2005) 2041.
[20] C.F.F. Karney, N.J. Fisch, Numerical studies of current generation by radio-frequency traveling waves, Phys. Fluids 22 (1979) 1817.
[21] C.F.F. Karney, N.J. Fisch, Current in Wave-driven Plasma, Phys. Fluids 29 (1986) 180.
[22] N.J. Fisch, Confining a tokamak plasma with rf-driven currents, Phys. Rev. Letter 41 (1978) 873.
[23] C.F.F. Karney, Fokker–Planck and quasi-linear codes, Comp. Phys. Rep. 4 (1986) 3–4.
[24] D.W. Ignat, E.J. Valeo, S.C. Jardin, Dynamic modeling of lower hybrid current drive, Nucl. Fusion 34 (1994) 837–851.
[25] C.F.F. Karney, N.J. Fisch, Efficiency of current drive by fast waves, Phys. Fluids 28 (1985) 116–126.
[26] P.T. Bonoli, R.W. Harvey, C. Kessel, F. Imbeaux, T. Oikawa, M. Schneider, E. Barbato, J. Decker, G. Giruzzi, C.B. Forest, S. Ide, Y. Peysson, A.E. Schmidt, A.C.C. Sips, A.P. Smirnov, J.C. Wright, Benchmarking of Lower Hybrid Current Drive Codes with Applications to ITER-relevant Regimes, PSFC/JA-06–33, Cambridge (MA), 2006.
[27] E. Barbato, F. Santini, Quasi-linear absorption of lower hybrid waves by fusion-generated alpha particles, Nucl. Fusion 31 (1991) 673.
[28] S. Ceccuzzi, E. Barbato, A. Cardinal, C. Castaldo, R. Cesario, M. Marinucci, F. Mirizzi, L. Panaccione, G.L. Ravera, F. Santini, G. Schettini, A.A. Tuccillo, Lower hybrid current drive for DEMO: physics assessment and technology maturity, Fusion Sci. Technol. 64 (2013) 748.
[29] A.A. Molavi Choobini, A. Naghidokht, Z. Karami, Simulation of lower hybrid current drive for DEMO, World J. Nucl. Sci. Technol. 4 (2014) 189–194.
[30] P.T. Bonoli, J. Parker, R. Ko, A.E. Schmidt, G. Wallace, J.C. Wright, C.L. Fiore, A.E. Hubbard, J. Irby, E. Marmar, M. Porkolab, D. Terry, S.M. Wolfe, S.J. Wukitch, The Alcator C-Mod Team, J.R. Wilson, S. Scott, E. Valeo, C.K. Phillips, R.W. Harvey, Lower hybrid current drive experiments on Alcator C-Mod: comparison with theory and simulation, Phys. Plasmas 15 (2008) 056117.
[31] D.W. Ignant, A.J. Redd, Lower Hybrid Simulation Code Manual, Plasma Phys. Laboratory, Princeton (NJ), 2000.
[32] L. Qi, X.Y. Wang, Y. Lin, Simulation of linear and nonlinear Landau damping of lower hybrid waves, Phys. Plasmas 20 (2013) 062107.
[33] G.T. Hoang, A. Bécoulet, J. Jacquinot, J.F. Artaud, Y.S. Bae, B. Beaumont, J.H. Belo, G. Berger-By, J.P.S. Bizarro, P. Bonoli, M.H. Cho, J. Decker, L. Delpech, A. Ekedahl, J. Garcia, G. Giruzzi, M. Goniche, C. Gormezano, D. Guilhem, J. Hillairet, F. Imbeaux, F. Kazarian, C. Kessel, S.H. Kim, J.G. Kwak, J.H. Jeong, J.B. Lister, X. Litaudon, R. Magne, S. Milora, F. Mirizzi, W. Namkung, J.M. Noterdaeme, S.I. Park, R. Parker, Y. Peysson, D. Rasmussen, P.K. Sharma, M. Schneider, E. Synakowski, A. Tanga, A. Tuccillo, Y.X. Wan, A lower hybrid current drive system for ITER, Nucl. Fusion 49 (2009) 075001.